fire

MDPI

Article

Forest Fire Regime in a Mediterranean Ecosystem: Unraveling the Mutual Interrelations between Rainfall Seasonality, Soil Moisture, Drought Persistence, and Biomass Dynamics

Nunzio Romano [1,2,*,†] and Nadia Ursino [3,†]

[1] Department of Agricultural Sciences, Division of Agricultural, Forest and Biosystems Engineering, University of Naples Federico II, Portici, 80055 Napoli, Italy
[2] The Interdepartmental Research Center for Environment (C.I.R.AM.), University of Naples Federico II, 80134 Napoli, Italy
[3] Department of Civil, Environmental and Architectural Engineering, University of Padova, 35131 Padova, Italy; nadia.ursino@unipd.it
* Correspondence: nunzio.romano@unina.it
† These authors contributed equally to this work and should be considered co-first authors.

Received: 21 July 2020; Accepted: 1 September 2020; Published: 3 September 2020

Abstract: Frequent and severe droughts typically intensify wildfires provided that there is enough fuel in situ. The extent to which climate change may influence the fire regime and long time-scale hydrological processes may soften the effect of inter-annual climate change and, more specifically, whether soil-water retention capacity can alleviate the harsh conditions resulting from droughts and affect fire regimes, are still largely unexplored matters. The research presented in this paper is a development of a previous investigation and shows in what way, and to what extent, rainfall frequency, dry season length, and hydraulic response of different soil types drive forest fires toward different regimes while taking into consideration the typical seasonality of the Mediterranean climate. The soil-water holding capacity, which facilitates biomass growth in between fire events and hence favors fuel production, may worsen the fire regime as long dry summers become more frequent, such that the ecosystem's resilience to climate shifts may eventually be undermined.

Keywords: ecohydrology; wildfire; drought; soil moisture; predator-prey model; Mediterranean climate; rainfall seasonality

1. Introduction

The southern European countries of the Mediterranean belt are characterized by significant intra-annual and inter-annual seasonality. This region is also known to be prone to wildfires, whose frequency and severity are intensified by prolonged periods with very little or no rainfall, also associated with extremely high temperatures, that reduce the amount of soil moisture in the uppermost soil horizons [1,2]. Even though every country in southern Europe has specific features, the above situation is encountered with different nuances in many zones worldwide where a Mediterranean-like climate occurs [3].

Relatively longer dry seasons recorded in recent years have triggered numerous fires all over the Mediterranean regions of Europe. Climatic seasonality also appears to have undergone some changes, but with different regional features. For example, the summer of 2018 broke several long-term meteorological records and was fairly wet in southern Europe, whereas it was hot and dry, together with some forest fires, in northern Europe. Added to the severity of fires recently occurring in the Mediterranean regions, the current situation has given rise to major concerns Europe-wide.

Determining the characteristics of the fire regime in a certain location requires the availability of long-term observations of fire records. However, systematic monitoring of fires is a relatively recent activity and only in the most favorable situations are a few decades of records available. Such a limited amount of data would not appear able to characterize a fire regime properly. However, there are clear perceptions and some evidence that, apart from possible anthropogenic disturbances, the oscillations of the frequency and magnitude of fires follow quite closely changes in local climatic conditions and alterations of the landscape and land-use patterns [4,5].

We put forward the idea that the evolution of a fire regime is driven more by local climatic conditions and land use than policy and socio-economic factors, and can therefore be conveniently forecasted by describing the main processes involved through a mechanistic eco-hydrological model while taking the local precipitation regime into account. In this paper, we discuss how this task can be performed and highlight the role of some more informative variables within the problem at hand while considering actual hydrological data observed in a zone in southern Europe.

Our modeling approach to the evolution of fire regimes and the relevant sensitivity analysis is discussed in the context of the region of Campania in southern Italy, a representative area of the Mediterranean belt. The area was chosen chiefly for the following reasons:

- Vast areas of Campania, some of which also have outstanding features from the landscape and heritage perspective, were ravaged by severe wildfires in 2017, such as the Vesuvius National Park and Cilento National Park as well as many hillsides on the renowned Amalfi Coast. Note that the Amalfi Coast and the Cilento National Park are both listed among "Cultural Landscapes" that UNESCO considers "World Heritage";
- Long time-series of weather records are available for Campania, together with detailed information on soil physical and hydraulic properties at the entire regional scale [6,7].

The influence of rainfall regime on fire-prone environment dynamics is manifold and operates at different time scales. Climate affects soil moisture availability and the growth of vegetation [8,9], hence fuel abundance. However, it also exerts a contrasting impact on the ignition and development of a fire. The typical Mediterranean climatic seasonality interacts with wildland fires negatively since a wildfire typically ignites toward the end of the dry season when fuel abounds and the environment is drier [10]. This is an extremely dangerous situation that can go easily out of control [11–13], mostly due in part to human negligence or malice, and in part to climate change [3,14,15]. As shown by Thuiller et al. [16], all these situations combine to generate conditions for the coexistence of different plant species. Moreover, soil wettability may be strongly reduced by severe fires, with consequences on interactions and feedbacks between soil moisture, vegetation, and local seasonal conditions [17].

Undoubtedly, burning biomass is the greater predator of almost any species [18], and therefore using a predator–prey model coupled with an ecohydrological approach seems a viable and efficient way to study the long-term evolution of a fire, accounting for the interactions that exist in Mediterranean environments between soil, vegetation, and climate [19–21]. An exceptional fire season is commonly associated with extremely dry environmental conditions and a result of a long-lasting complex process of fuel production over many growing seasons (in the absence of fire). The interplay between fire, vegetation, and soil characteristics may alter the availability of soil moisture during the growing season, and ultimately vegetation growth and fuel production, thus affecting the hydrological cycle overall.

The fire paradox of self-sustaining Mediterranean fire-prone forests is often associated with the display of a chaotic-type fire regime that is characterized by a highly variable return period and, especially at high vegetation growth rates, by complex non-linear dynamics within the space of relevant model parameter values [22]. Far from this chaotic-type regime, different dynamics can be envisioned under persistent climate change scenarios [23], or substantial land-use changes [24]. These situations represent the environmental risk of a shift in the ecosystem considered, apart from the likely occurrence of an isolated big fire event. The latter type of event is instead the objective of provisional conceptual models of fire risk assessment which, however, are not considered here and refer to time scales with an order of magnitude very different from those (roughly hundreds of years) assumed in the present study.

By applying a conceptual eco-hydrological fire model to the case study of the southern Italian region of Campania, we address the question of whether observed climate change could drive the forest ecosystem far from its characteristic, self-sustaining fire regime and to what extent soil-mediated water cycling may oppose such shifts in the ensuing decades. In this study, we focus on the soil water holding capacity and drought persistence that are hydrological features mostly affecting fuel production. Rainfall data are statistically analyzed to infer typical climate scenarios. Measured soil properties are used to parameterize the model and obtain frequency histograms of soil moisture and forest biomass density. The results demonstrate that the soil water holding capacity, facilitating biomass growth in between fire events, and thus favoring fuel production, may intensify the fire regime when long dry summers become more frequent.

2. Overview and Rationale of the Simulation Approach

The interconnection between soil moisture and biomass balances is modeled through a set of five partial differential equations: one for the soil moisture (S) balance, two for the balance of biomass density, which includes both trees (B_u) and shrubs (B_l), and two for the burning tree and shrub densities (R_u and R_l, respectively). The subscripts "u" and "l" refer to the upper (i.e., the overstory) and lower (i.e., the understory) vegetation, respectively. We further improved the previous version of the model developed in study by Ursino and Romano [24] by assuming that:

- Rainfall is a Poisson stochastic process with parameters depending on the season of the year;
- Dry and rainy season dynamics are different: no fire event occurs during the rainy season when the vegetation is dormant, i.e., is lying in a state of minimal metabolic activity;
- Soil hydraulic characteristics may be modified for a certain time lapse after a fire depending on its severity.

Simulation models have become a standard tool for analyzing even complex environmental ecosystems, and the bucket-type hydrological model described in Section 2.1 below is used extensively and successfully for both conceptual analyses and practical applications dealing with soil moisture and vegetation dynamics [9]. Small changes to this model, with respect to a more classic expression one can find in the literature, have been introduced in this paper to better account for some Mediterranean features, such as the different rainfall interception by the understory and overstory vegetation as well as the partitioning of the evapotranspiration fluxes between soil evaporation and plant transpiration. However, these changes certainly do not invalidate this renowned hydrological model.

The link between our hydrological model and the fire-prone biomass equation, as presented in Section 2.2, is not commonly found in the literature because it underpins the idea that fire is the result of long-lasting complex processes. Our view of the problem is obviously in contrast to the picture provided by simplistic instantaneous fire danger indices (e.g., the Fire Weather Index; [25]) often employed in forest management to identify fire risk maps and emergency measures. In the present study, we instead present sensitivity analyses to emphasize the importance of the complex interaction between vegetation biomass and soil moisture dynamics. Given the lack of historical awareness of the relevance of long-term processes on the establishment of a fire regime, at present we can only envision an on-site validation of our new approach. However, a specific feature of the sensitivity analyses presented in this paper is that the values of the input variables and parameters required by the model are based on actual observations and sound and verified experimental procedures.

2.1. Modeling Soil Moisture Dynamics

Soil moisture dynamics is described by the following non-linear differential equation of water balance, written for a hydrologically effective soil profile of thickness Z [26,27]:

$$n\,Z\,\frac{dS(t)}{dt} = \pi[S(t),\,t] - \chi[S(t)], \tag{1}$$

where t is time (in day), n is the vertically averaged soil porosity, and S ($0 \leq S \leq 1$) is relative soil moisture content (expressed as $S = \theta/n$, i.e., the volumetric soil-water content, θ, normalized by soil porosity, n) averaged over the entire depth Z (in mm) of the soil control volume. We attach a more functional than physical meaning to the soil control volume of depth Z as it represents the hydrologically active, uniform soil profile where the evapotranspiration process plays a dominant role. Equation (1) is a stochastic model of soil moisture dynamics at a point since we treat precipitation (P) as a Poisson stationary random process characterized by the inter-arrival time, τ (in days), between independent precipitation events, and the daily precipitation depth, p (in mm), and duration, t_p (in day) [8].

The right-hand side of Equation (1) comprises the following incoming and outgoing fluxes:

$$\pi[S(t),\ t] = P(t) - CI(t) - Q[S(t), t], \tag{2}$$

$$\chi[S(t)] = E[S(t)] + T[S(t)] + L[S(t)], \tag{3}$$

where P is precipitation, CI is canopy interception, Q is surface runoff, E and T are actual evaporation and transpiration, respectively, and L is leakage (i.e., the drainage losses) from the lower boundary of the soil profile. The flux in Equation (1) has dimension LT^{-1} and, unless otherwise specified, the linear dimension has units of "mm", whereas the time dimension has units of "days".

Actual rates of soil evaporation, E, actual plant transpiration, T, and leakage, L, are considered only as a function of the spatial average soil saturation (S) and season of the year, whereas surface runoff, Q, is generated according to the saturation-excess or infiltration-excess mechanisms depending on the soil condition at time t, which is influenced by previous fire occurrence under the assumption that the effect of fire on soil properties (such as a reduction in soil infiltration capacity due to the loss of soil wettability after the formation of a water repellent uppermost soil layer) lasts one year. Actually, variable $\pi[S(t), t]$ of Equation (2) includes the portion of precipitation (P) that infiltrates into the control volume through the soil surface, after the subtraction of canopy interception (CI) and surface runoff (Q) if they both occur.

In the absence of a fire event, the interception by vegetation canopy is modeled rather simplistically such that $ci(t) = \min\{\Delta, p(t)\}$, where Δ (in cm) is a threshold value of precipitation depth below which no water reaches the soil surface [9,28]. Crown fire reduces the interception capacity of the overstory, also in accordance with Caylor et al. [29] who suggested that the amount of interception is proportional to the leaf area index and the number of canopies present. The threshold is calculated as follows:

$$\Delta = \Delta_u B_u + \Delta_l B_l, \tag{4}$$

where B_u and B_l are the biomass density of the upper and lower vegetation layers, respectively. Therefore, the depth of net rainfall, $r'(t)$, that reaches the soil surface is as follows:

$$\begin{cases} r'(t) = 0 & if\ p(t) \leq \Delta \\ r'(t) = p - \Delta & if\ p(t) > \Delta \end{cases}. \tag{5}$$

Obviously, when no vegetation interception occurs and/or just after a fire event (i.e., when Δ=0), the net rainfall (i.e., throughfall) is $r' = r = p$ (see Table A1).

The infiltration capacity of soil, $f(t)$, undergoes a substantial reduction after a fire event [30,31]. The Hortonian process for overland flow generation occurs when rainfall intensity $j(t) = r'(t)/t_p(t)$ exceeds soil infiltration capacity, $f(t)$, with $t_p(t)$ being the duration of the rainfall event. Therefore we use the following relation:

$$i[S(t), t] = r'(t) - q = min\Big\{r'(t),\ f(t) \cdot t_p(t),\ nZ[1 - S_0(t)]\Big\}, \tag{6}$$

where S_0 is the relative soil moisture in the control volume at the beginning of a rainfall event.

Consequently, overland flow (q) can be generated by either saturation-excess or infiltration-excess mechanisms and is computed as follows:

$$q[S(t),t] = \begin{cases} 0 & ;\ if\ r'(t) \le min\left\{f(t)\cdot t_p(t),\ nZ[1-S(t)]\right\} \\ r_{exc}(t) = r'(t) - min\left\{f(t)\cdot t_p(t),\ nZ[1-S(t)]\right\} & ;\ if\ r'(t) > min\left\{f(t)\cdot t_p(t),\ nZ[1-S(t)]\right\} \end{cases}. \quad (7)$$

Severe fires, which typically ignite at the end of summer, can alter the soil structure and hence increase the imperviousness of recently burned soils. This will limit the amount of rainfall that infiltrates over the subsequent rainy period (autumn season), and therefore replenishes the soil profile and later on becomes available for vegetation [17,31–36].

The biomass density of the upper and lower vegetation layers, namely B_u and B_l, is limited by the local environmental conditions other than soil moisture availability and fire to the carrying capacity k_u and k_l, respectively. The carrying capacities of the two layers are used to derive dimensionless biomass density B^*_u=B_u/k_u and B^*_u=B_l/k_l.

The impact of a fire on soil properties lasts for about one year after fire [37–41]. With R^*_u and R^*_l being the dimensionless burning biomass density, i.e., the maximum amount of biomass burned normalized to the carrying capacity according to the living biomass density (see [24]), our modeling approach considers that, any time the during the one-year time lag (t–1yr; t), the partitioning of precipitation into overland flow is affected by a reduced soil infiltration capacity according to the following expression:

$$f\left[S(t),\ t,\ R^*_u,\ R^*_l\right] = f_0 \cdot g\left(R^*_u,\ R^*_l\right), \quad (8)$$

where f_0 is soil infiltration capacity in the absence of fire and:

$$g(t) = \frac{R^*_u + R^*_l}{R^*_u + R^*_l + K_\phi}. \quad (9)$$

The parameter K_ϕ depends on the soil composition and vegetation cover, and accounts for the degree of imperviousness induced by the fire event. Ursino and Rulli [23] presented an extensive sensitivity analysis of the fire regime for K_ϕ ranging from 0 to K_ϕ>>1 (actually, this parameter is set at 1 in the present study; see Table A1 in the Appendix A).

With a view to the modeling objectives of this study, namely to evaluate the impact of hydrological processes on fire regime, we follow Guswa et al. [26] who suggested separating the actual evaporation at the soil surface, $E(S)$, from the actual transpiration by plants, $T(S)$. These two variables are computed as follows:

$$E(S) = \begin{cases} 0 & S \le S_h \\ \left(\frac{S-S_h}{S^{**}-S_h}\right)^{e_1} \times E_{max} & S_h < S < S^{**} \\ E_{max} & S \ge S^{**} \end{cases}, \quad (10)$$

$$T_{u,l}(S) = \begin{cases} 0 & S \le S_{wp_{u,l}} \\ \left(\frac{S-S_{wp_{u,l}}}{S^*_{u,l}-S_{wp_{u,l}}}\right)^{t_1} \times T_{max_{u,l}} & S_{wp_{u,l}} < S < S^*_{u,l} \\ T_{max_{u,l}} & S \ge S^*_{u,l} \end{cases}. \quad (11)$$

In Equation (10), S^{**} is a soil moisture threshold below which a reduction in evaporation rate occurs [42], whereas S_h is the so-called hygroscopic moisture content, namely the average soil moisture content when soil suction head at the soil-atmosphere interface ($|\psi_{s\text{-}a}|$) is low enough for evaporation from the soil surface to cease. Soil suction head $|\psi_{s\text{-}a}|$ is often set at a value ranging from $150{\cdot}10^3$ to $500{\cdot}10^3$ cm, and we posit $|\psi_{s\text{-}a}|$=$500{\cdot}10^3$ cm in the present study. In Equation (11), S_{wp} is soil moisture at permanent wilting condition (i.e., the wilting point) and S^* is soil moisture at incipient stomatal closure, and we assume that both these parameters take on different values for overstory (e.g., olive or

chestnut trees) or understory (e.g., shrubs). The exponents e_1 and t_1 featuring in Equations (10)–(11) account for possible nonlinearity in these relationships and here are both set equal to 1.0 [19]. Values for these parameters are reported in Tables A3 and A4 in the Appendix A.

Evapotranspiration of the two vegetation types is computed as follows:

$$ET(B_u, B_l, S) = E(S)\left[1 - max\left(\frac{B_u}{k_u}, \frac{B_l}{k_l}\right)\right] + T_u(S)\frac{B_u}{k_u} + T_l(S)\frac{B_l}{k_l}, \quad (12)$$

where $E(S)$ is actual evaporation flux estimated according to Equation (10), but note that this variable takes on different values during the wet or dry season because vegetative activity is assumed to take place during the dry season [20]. See Table A5 in the Appendix A for the relevant parameter values used in these equations.

The vertically lumped bucket model assumes that the drainage rates occur under the condition of the unit gradient of the total hydraulic potential and are expressed as a function of the soil saturated hydraulic conductivity, K_s, as follows:

$$L(S) = \begin{cases} 0 & S \le S_{fc} \\ K_s S^{\gamma} & S_{fc} < S \le 1 \end{cases}, \quad (13)$$

where γ is the soil-pore/connectivity parameter and S_{fc} is the relative soil moisture at "field capacity" [20]. The determination of the S_{fc} value deserves some comments. Since the model control volume is not an actual (mostly, layered) soil profile, but rather an equivalent uniform soil, in this study we take advantage of the recent findings made by Nasta and Romano [43], who set up a functional evaluation and an analytical procedure to identify the effective value of soil moisture at field capacity in the case of an actual layered soil profile.

2.2. The Modified Predator–prey Model for Fire Dynamics

Predator–prey interactions are often used to interpret density-dependent limiting factors occurring in a certain environment, and the related analyses have proved to be quite successful especially in behavioral ecology studies to describe the patterns of time variations of the investigated variables or species [44,45]. Following suggestions made by some researchers, predator–prey models rapidly attracted the attention of researchers, managers, and professionals who had to deal with vegetation fires and their dynamics [46]. One feature of a predator–prey model that interested us was its potential to serve as a stochastic tool for a system of two competing attributes, which makes it very suitable to be coupled with the stochastic description of soil moisture dynamics offered by Equation (1).

Previous predator–prey models developed to investigate fire regimes were based on average annual precipitation and therefore simulated annual water balance [23,24]. Instead, given the chief aims of the present study, the stochastic precipitation variables, i.e., p, t_p, and τ, are independent and exponentially distributed with season-dependent averages. During the wet or dry season, the average precipitation amount, the reciprocal of precipitation duration, and inter-arrival time are denoted by the symbols ζ, δ, and λ, respectively, with the subscript "*wet*" or "*dry*" that refers to the specific season considered (see Table 1). As the wet seasons of Mediterranean climates are typically out-of-phase with vegetative growing periods, the amount of precipitation potentially involved in the water balance is restricted approximately to the amount of water that is stored in the soil profile at the beginning of the growing season plus the rainfall during the dry season. Note that the values for variable I can undergo a reduction over the first few years following a fire event because a burning event usually creates a nearly impermeable soil layer that reduces the amount of water entering the soil control volume.

Table 1. Seasonal rainfall parameters of the Poisson rectangular pulse (PRP) model used in the sensitivity analyses: (ζ (in mm) = mean rainfall depth (p); λ (in day^{-1}) = reciprocal of the mean rainfall interarrival time (τ)); δ (in day^{-1}) = reciprocal of the mean rainfall duration (t_p). *ND* is the number of days in the wet or dry season and *P* is cumulative precipitation (yearly or seasonal). The hydrological year starts on 1st April and on this day we assume that the dry season begins.

Scenario	ND_{wet}	ζ_{wet}	λ_{wet}	δ_{wet}	P_{wet}	ND_{dry}	ζ_{dry}	λ_{dry}	δ_{dry}	P_{dry}	P_{year}
	day	mm	day^{-1}	day^{-1}	mm	day	mm	day^{-1}	day^{-1}	mm	mm
S1-A	183	10.65	0.40	6.0	779.6	182	8.487	0.25	8.0	386.2	1165.8
S1-B	120	10.62	0.40	6.0	511.2	245	8.487	0.25	8.0	519.8	1031.0
S2-A	183	6.59	0.27	6.0	325.6	182	6.670	0.19	8.0	230.6	556.2
S2-B	120	6.59	0.27	6.0	213.5	245	6.670	0.19	8.0	310.5	524.0

Frequency and magnitude of fire are dictated by fuel availability and environmental dryness, hence ultimately by climate indirectly through its influence on vegetation growth and directly under conditions of the high flammability of fuel. To reduce the number of dependent variables to only two variables per species (living and burning biomass density), the burning biomass is the "*predator*" and the living biomass is the "*prey*", even though it is the dry matter that becomes fuel for a fire at the end of the dry season. The amount of fuel available every year is assumed to be proportional to the living biomass.

The four dimensionless balance equations that determine the predator–prey dynamics of the living and burning trees and shrubs (upper and lower layer or overstory and understory, respectively) are the following:

$$\begin{array}{l} \frac{\partial B_u}{\partial t} = G_u(S, B_u) - F_u(S, B_u, R_u, R_l) \\ \frac{\partial R_u}{\partial t} = F_u(S, B_u, R_u, R_l) - D_u(R_u) \\ \frac{\partial B_l}{\partial t} = G_l(S, B_l, B_u) - F_l(S, B_l, R_u, R_l) \\ \frac{\partial R_u}{\partial t} = F_l(S, B_l, R_u, R_l) - D_l(R_l) \end{array} . \quad (14)$$

During the dry season, G_u and G_l are biomass logistic growth functions. At very low values of S, corresponding to prolonged conditions of water scarcity and droughts in the ecosystem, vegetation does not grow and does not produce fuel. At higher S values, instead, it is not flammable. The two situations mentioned above are synthesized through the following analytical expressions:

$$\begin{array}{l} G_u(S,\ B_u) = r_u B_u\left(1 - \frac{B_u}{k_u}\right) \cdot f(S) \\ G_l(S, B_l,\ B_u) = r_l B_l\left(1 - \frac{B_l}{k_l}\right) \cdot f(S) - \alpha\ B_u \frac{B_l}{k_l} \end{array} . \quad (15)$$

The net primary productivity (NPP) of Mediterranean forest ranges between 0.5 and 1.5 kg·m^2·yr^{-1}, whereas the NPP of Mediterranean scrubland ranges between 0.3 and 0.6 kg·m^2·yr^{-1} [47]. The parameters r_u and k_u, as well as r_l and k_l, characterize the vegetation growth rate (r_u and r_l) and carrying capacity (k_u and k_l) over their area of occupancy, according to the referred literature data. The biomass densities B_u and B_l represent each species' abundance, whereas the burning biomass density (R_u and R_l) is responsible for the impact of fire on hydrological processes.

In Equation (15), r_u is proportional to yield and the ratio $T_u/T_{max,u}$, whereas r_l to species-specific yield and $T_l/T_{max,l}$. Actual transpiration is calculated as a function of relative soil moisture soil saturation through Equation (11) and accounts for the lack of biomass production due to the water stress occurring during very dry years.

When enough fuel is available and the environment is sufficiently dry, fire develops as soon as $F_{u,l}<D_{u,l}$. The burning biomass of each layer attacks the living biomass of both layers, igniting a fire with severity that is inversely proportional to the soil moisture:

$$\begin{array}{l} F_u(S,B_u,R_u,R_l) = \left[\beta_u \frac{B_u}{(B_u+h)} R_u + \gamma_u \frac{B_u}{(B_u+h)} R_l\right] \cdot g(S) \\ F_l(S,B_l,R_u,R_l) = \left[\beta_l \frac{B_u}{(B_l+h)} R_l + \gamma_l \frac{B_l}{(B_l+h)} R_u\right] \cdot g(S) \end{array}, \quad (16)$$

where:

$$g(S) = \begin{cases} 0 & S > S_{fire} \\ \left(1 - \frac{S}{S_{fire}}\right)^{\chi} & S \le S_{fire} \end{cases}. \quad (17)$$

Soil moisture content (S) is interpreted as a proxy of the moisture content of the plant biological tissues that inhibit fire development [48–52]. High parameter χ could be used for less drought-tolerant species, drying out quickly when soil moisture availability decreases. Even moderately low soil moisture values favor the development of fires. Low parameter χ restricts the development of fire only to very dry conditions, representing the behavior of more drought-tolerant and less flammable species. When soil moisture exceeds the threshold S_{fire}, then no fire can develop.

Burning plants of the two layers become extinct at a given rate:

$$\begin{array}{l} D_u(R_u) = \delta_u R_u \\ D_l(R_l) = \delta_l R_l \end{array}. \quad (18)$$

The symbols δ_u and δ_l are the fire extinction rates in the tree and shrub layers, respectively, that are typical of the Mediterranean ecosystem under consideration. The dynamics of burning species are much faster than those of living species. Parameter values are chosen according to previous literature contributions and specified in Table A5 of the Appendix A. The vegetation is dormant during the rainy season and $G_u = G_l = 0$ and fire does not ignite spontaneously, namely $F_u = F_l = D_u = D_l = 0$.

2.3. Scenarios for Sensitivity Analysis

Equation (1) requires as input information the daily precipitation that indirectly drives biomass growth and likely fire occurrence through dryness and fuel abundancy. Within Campania, reference was made to the weather stations of Salerno and Gioi Cilento. Salerno is a city by the sea and its station has long time-series of daily rainfall data that are employed here as suitable information for the Amalfi Coast and the Vesuvius National Park. Instead, the village of Gioi Cilento is situated in the Cilento, Vallo di Diano and Alburni National Park.

The weather station of Salerno (X-UTM: 479,039 m; Y-UTM: 4,503,239 m) is located at 13 m above sea level (a.s.l.), whereas the weather station in the village of Gioi Cilento (X-UTM: 518,534 m; Y-UTM: 4,460,028 m) is located at 668 m a.s.l. Therefore, the two stations can be viewed as representative of precipitation regimes occurring near the coastal areas and in hilly zones, respectively, of the region in question. These stations have values of the seasonality index (SI; [53]) in the range 0.40–0.59, meaning that the precipitation regime is rather seasonal with a short dry season.

To provide the reader with a clear understanding and a less biased perspective of observed dry spells in a typical zone of Mediterranean Europe, we computed the Standardized Precipitation Index (SPI; [54]) for several weather stations located in the southern Italian region of Campania. Computing SPI is highly recommended by the World Meteorological Organization to characterize the meteorological drought, and the use of a standardized indicator helps compare the outcomes from various stations. SPI values quantify the precipitation deficit (negative values) or surplus (positive values) with respect to the median value in the observed period. According to the SPI classification of drought conditions, a period is severely dry for SPI values ranging from −1.5 to −1.99, whereas it is extremely dry when SPI values are lower than −2.00.

Figures 1 and 2 depict the three-month standardized precipitation index (SPI-3) for the two weather stations of Salerno and Gioi Cilento by using the daily rainfall data recorded from 1920 to 2018 at these points. No rainfall data were recorded at these stations during the Second World War and for a few years after its conclusion. We selected an accumulation period of three months for SPI since this time scale seems to reflect more medium-term soil moisture conditions and takes seasonal precipitation regime into due account. In both bottom panels of Figures 1 and 2, the line segment in magenta connects the median values of SPI-3 and highlights the occurrence of more frequent precipitation anomalies slightly after the year 1990 (in a few cases close to -1.0 for Gioi Cilento and even greater than -1.0 for Salerno). Moreover, in the recording period from 1990 to 2018, the median dry anomalies are greater than the wet ones for both Salerno and Gioi Cilento weather stations.

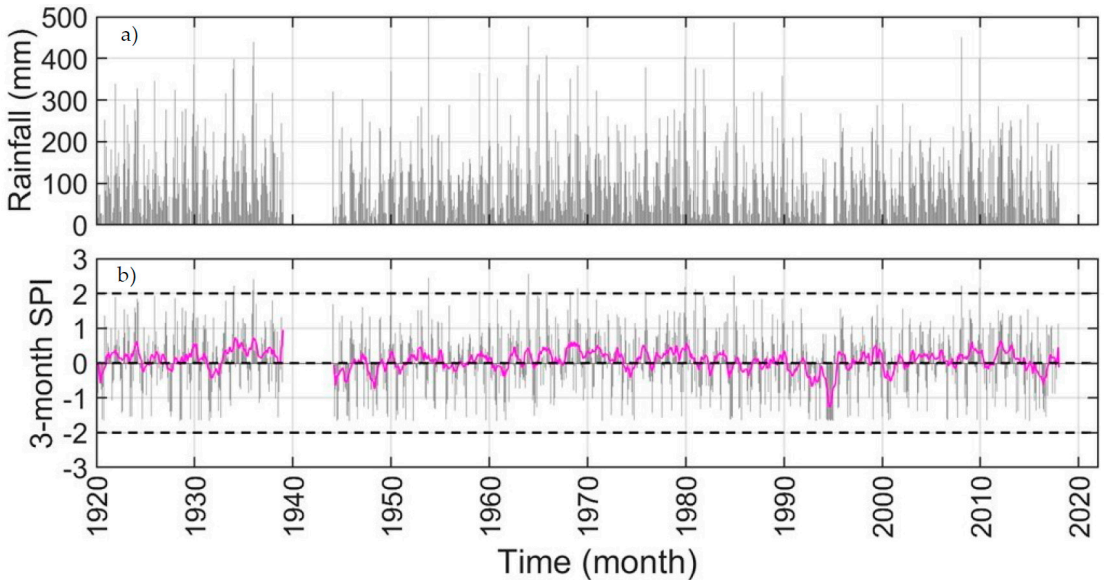

Figure 1. Monthly rainfall (**a**) and Standardized Precipitation Index (SPI)-3 (**b**) time series for the period 1920–2018 recorded at the Salerno weather station.

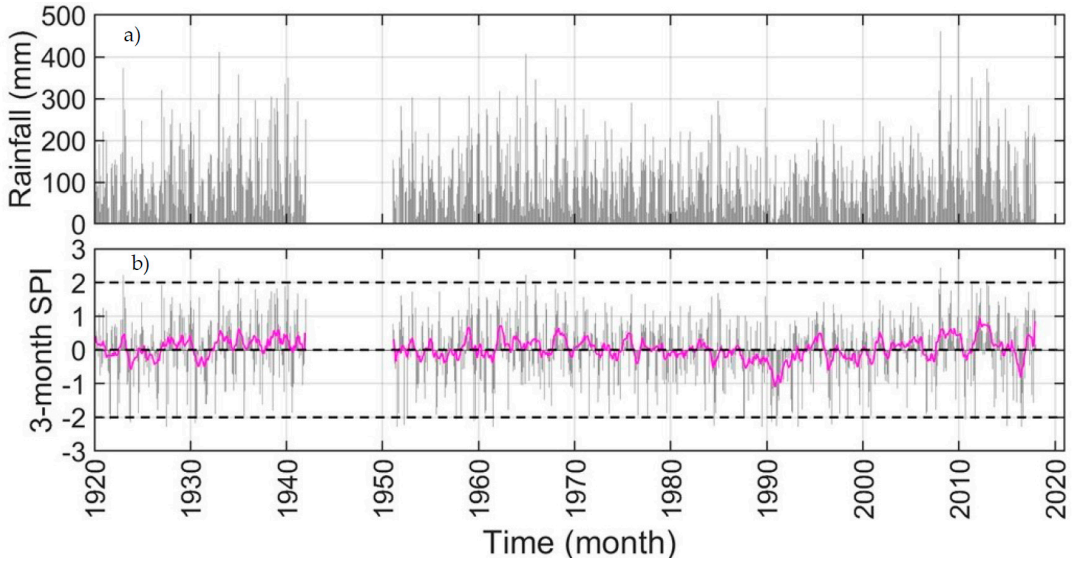

Figure 2. Monthly rainfall (**a**) and SPI-3 (**b**) time series for the period 1920–2018 recorded at the Gioi Cilento weather station.

The impact that the typical seasonality of a Mediterranean precipitation regime may exert on the time evolution of the occurrence of wildfires is evaluated by identifying two different precipitation

scenarios, referred to as S1 and S2. It is worth noting that the individual parameter values attached to these seasonal precipitation regimes rely on actual long-term rainfall records available from about 250 weather stations located throughout Campania and can be conveniently viewed as representative of rainfall situations occurring in differently located zones of the study region (see Table 1).

To account for intra-annual rainfall seasonality, both scenarios S1 and S2 in Table 1 refer to a conventional hydrological year, starting on April 1st. Based on datasets available in the literature (e.g., [7,20]), precipitation scenario S1-A has a mean annual precipitation (P_{year}) of more than about 1150 mm/yr, which can be considered as representative of average conditions occurring in some Mediterranean hill zones. Instead, precipitation scenario S2-A has a mean annual precipitation of approximately 550 mm/yr which occurs more frequently in southern, coastal zones of this region. Table A2 reports the Poisson parameters pertaining to these two precipitation scenarios. Both scenarios S1-A and S2-A refer to a hydrological year that is split into a dry season, lasting six months (namely 182 days from April to September of a certain year), typically characterized by fewer precipitation events and vegetation re-growth, and a wet season, lasting the other six months (namely 183 days from October to March of the subsequent year), when vegetation is virtually dormant and typically characterized by more precipitation events. Scenarios S1-B and S2-B use the same Poisson parameters as the previous cases, but refer only to an arbitrary (albeit realistic) increase in the number of days (NDdry) from 183 to 245 over a dry period (i.e., a dry period lasting nearly 8 months). It should be pointed out, however, that we made the simplistic assumption that the same Poisson parameter values are held in the cases considered.

To overcome the limits of simulations based on only one realization of the rainfall process over the observation time of 50 years, we further address the probability of achieving a certain forest composition under prescribed stochastic climate conditions by analyzing much longer simulation runs (e.g., 10,000 runs) within a Monte Carlo approach. We addressed the frequency histograms of the main dependent variables for both scenarios S1 and S2 as well as for the two soil types (loam and sandy clay loam soil, respectively).

2.4. Initial and Boundary Conditions

To lower as much as possible the influence of the initial condition on the model outputs, our model is first run for a period of 200 years. The dynamic equilibrium reached by the system at the end of the so-called spin-up period is then used as the initial condition for the next 50 years of simulation outputs, for scenario S1, and for the next 100 years in the case of scenario S2, to demonstrate what would be the reference or "physiological" fire regime under stationary eco-hydrological and environmental conditions. The fire regime over the 50 simulation years is influenced by the simulated rainfall over that time and will not be the same in the next 50 years. Once again, we should point out that the modeling exercise described here is run to highlight to what extent the dynamics of hydrological processes may affect the fire regime.

3. Results

Among the hydrological processes which most affect fuel production, accumulation, and dry out, we discuss the following: soil-water holding capacity and drought persistence. Specifically, we examine to what extent soil moisture availability, resulting from rainfall infiltration and biomass dynamics, exerts effects on the wildfire regime.

Simulations are run for two differently-textured soils: a loam (L) and a sandy clay loam (SCL) soil, whose parameters of the Campbell hydraulic relations [55] are reported in Table A2 of the Appendix A. For both soils, the effective control volume has a depth Z = 40 cm, whereas for all the simulation runs the initial state in the soil control volume is the soil moisture value at "field capacity" (θ_{fc}) computed as discussed in Section 2.1 (see Table A3 in the Appendix A).

Figure 3 refers to the precipitation scenario S1 and shows the variations over 50 years in biomass density for the overstory (black line) and understory (blue line) in the case of a hilly Mediterranean

environment. A fairly sharp drop in biomass density, which abruptly reduces or even sets this variable to zero, indicates the occurrence of a fire event. Instead, small fluctuations in the biomass density patterns indicate the effect of seasonality on species growth. Note that trees approaching forest canopy closure cause a slow decline in shrub density because they outcompete shrubs for light. This also explains in part the relative patterns with time shown in all plots of Figure 3 between the overstory and understory density.

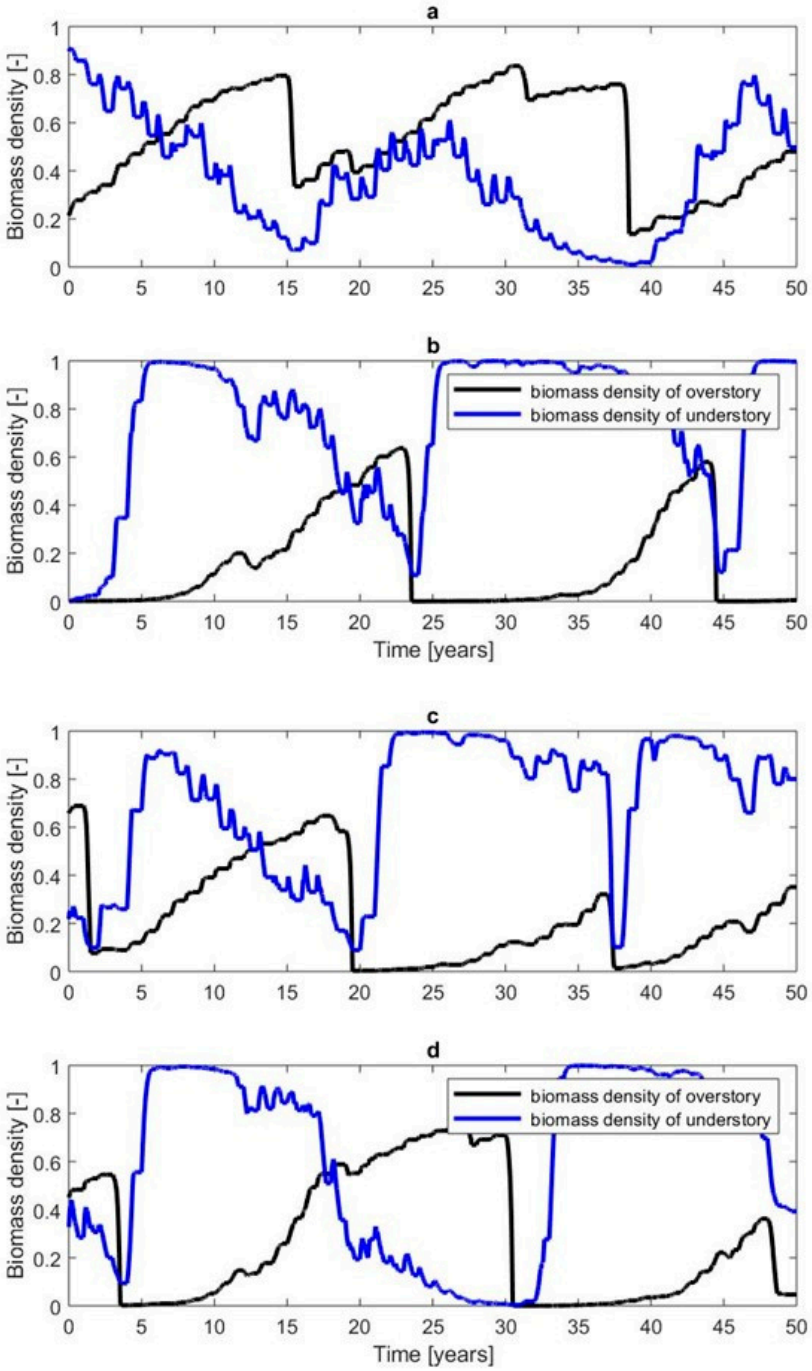

Figure 3. Variation in biomass density vs. time for the overstory (B_u; black line) and understory (B_l; blue line) vegetation. The top panels refer to scenario S1-A and the bottom panels scenario S1-B. Results shown in the left panels (**a**,**b**) pertain to the loam (L) soil, whereas those in the right panels (**c**,**d**) concern the sandy clay loam (SCL) soil.

The top panels (Figure 3a,c) refer to scenario S1-A (with a dry period lasting 183 days) for the loam (Figure 3a) and sandy clay loam (Figure 3c) soil, respectively. The bottom panels (Figure 3b,d), instead, refer to scenario S1-B (with a longer dry period lasting 245 days), again for the loam (Figure 3b) and sandy clay loam (Figure 3d) soil, respectively. Understory vegetation (e.g., shrub species depicted by the blue lines) reflect more closely the superimposed rainfall seasonality and the changes in dry spells, burning when their dry matter is abundant and attaching fire to trees which experience mild intensity fire events. The most intense fire events occur when the overstory biomass density is very high and shrubs are almost absent. Fire intensity increases with aridity and frequency of fire decreases. After any fire event, the first re-sprouting species are in the understory.

According to climate and soil texture, the faster the understory recovers, the faster the new fuel accumulates and the shorter the time lag to the next fire event. The latter feature is more evident in the case of scenario S1-A (plots 3a and 3c), which is characterized by the highest average annual precipitation (P_{year} = 1165.8 mm/yr).

Overall, the temporal fluctuations of the overstory density (black lines) indicate that this plant type is less affected by the seasonal conditions in question. Fires are never periodic; rather, their occurrence shows a chaotic behavior that is typical of Mediterranean forests (again more evident for scenario S1-A). This chaotic behavior of fire occurrence depends somewhat on the precipitation regime, but should be mainly attributed to the nonlinearities that characterize the entire modeled system [23].

The typical six-month duration of a rainy season in a hilly zone of the Mediterranean region (scenario S1-A in Figure 3a,c) leads to relatively frequent fires. However, the average soil hydraulic behavior of an area also plays a certain role since we observe that a relatively larger number of fires occur in the case of the loam (L) soil (Figure 3a). The greater soil-water holding capacity of L (see Figure 3a) than the SCL soil allows the former soil type to guarantee a relatively good recovery of both overstory and understory vegetation that coexist even after a fire event. Instead, the soil hydraulic response of the sandy clay loam (SCL) soil (see Figure 3c) does not adequately support the recovery of the overstory vegetation. If a prolonged dry period occurs (i.e., 245 days) even in zones with relatively high yearly rainfall (scenario S1-B in Figure 3b,d), fire events are rare but catastrophic, leading to the destruction of both overstory and understory. These features are observed irrespective of the average hydraulic behavior of the soils considered.

Figure 4 is similar to Figure 3 above, albeit showing the results for precipitation scenario S2, which might be viewed as characteristic of a Mediterranean river basin under more arid climatic conditions. Model outputs for this scenario S2 cover 100 years. As compared to the previous scenario S1 (see Figure 3), it is noticeable that for scenario S2 depicted in Figure 4, soil hydraulic properties now play a major role in determining the ability of the system to recover after any fire event. In the case of loamy (L) soil (Figure 4a,b), the understory, which recovers after a short time, reaches a relatively high density because trees are absent for a long time, and exploits the scarce precipitation exclusively. By contrast, the overstory finds it difficult to recover after a fire event; hence in this case we observe a lower number of fires. In the case of the sandy clay loam (SCL) soil and a rainy season lasting six months (see Figure 4c), the overstory recovers slightly better because the fires are less intense, but the understory density varies more erratically since it is not sufficiently sustained by the amount of water stored in profile of this soil type. Although the increase in fire frequency is, for both soil types, similarly linked to the precipitation regime, a shorter rainy season lasting four months (see Figure 4b,d; [56]) exacerbates the frequency and intensity of fires.

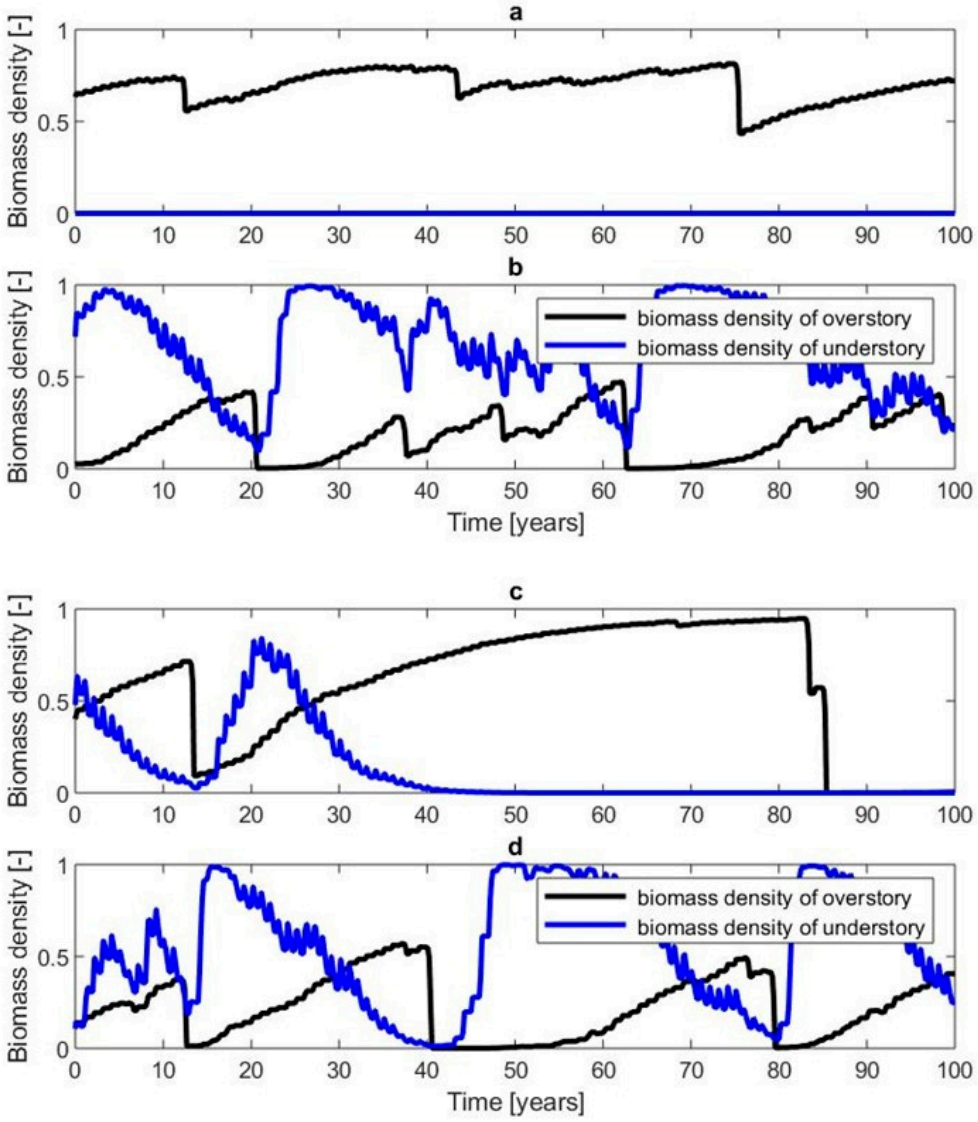

Figure 4. Variation in biomass density vs. time for the overstory (B_u; black line) and understory (B_l; blue line) vegetation. The top panels refer to scenario S2-A and the bottom panels scenario S2-B. Results shown in the left panels (**a**,**b**) pertain to the loam (L) soil, whereas those shown in the right panels (**c**,**d**) concern the sandy clay loam (SCL) soil.

The temporal dynamics of the biomass densities over relatively long periods clearly reveal that the combinations of soil and climate can affect the overall features of a fire regime, whether somewhat periodic or chaotic, or even the absence of fire. In the scenarios shown herein, the fire regime remains chaotic. This is a somewhat expected "physiological" characteristic of wildfire in Mediterranean regions [22].

The panels in Figure 5 depict the frequency histograms for precipitation scenario S1 (high yearly rainfall) and a loam (L) soil. From perusal of both top and bottom panels depicting the relative soil moisture, S, the presence of evident bimodality may be noted in the frequency histograms. The superimposed longer-lasting spell (actually, an increase) in the dry weather (i.e., moving from scenario S1-A to S1-B) undoubtedly results in the slightly different frequency levels for S in these two (left) plots, but does not seem to affect the general results to a great extent. Indeed, it is the seasonality of the precipitation regime that dictates the bimodal (double-peaked) features of the probability distribution of the relative moisture content in soil. As already observed by Romano et al. [20], we

also detected a greater frequency peak when the system undergoes wetter weather conditions. As for the central and right panels that depict the frequency distributions of vegetation density, they both reflect how the fire dynamics affect an ecosystem and reveal the presence of sharp peaks at zero. This occurrence corresponds to a quiescent period of both overstory and understory vegetation after a fire event. Instead, the peaks in the histograms when the understory density is equal to 1 (right panels of Figure 5) confirm the greater resilience of shrub species compared to tree species. The overstory vegetation has highly skewed histograms and seems more greatly affected by the assumed increase in the dry period, with the frequency peak at zero in the case of scenario S1-B being about 50% greater than that of scenario S1-A.

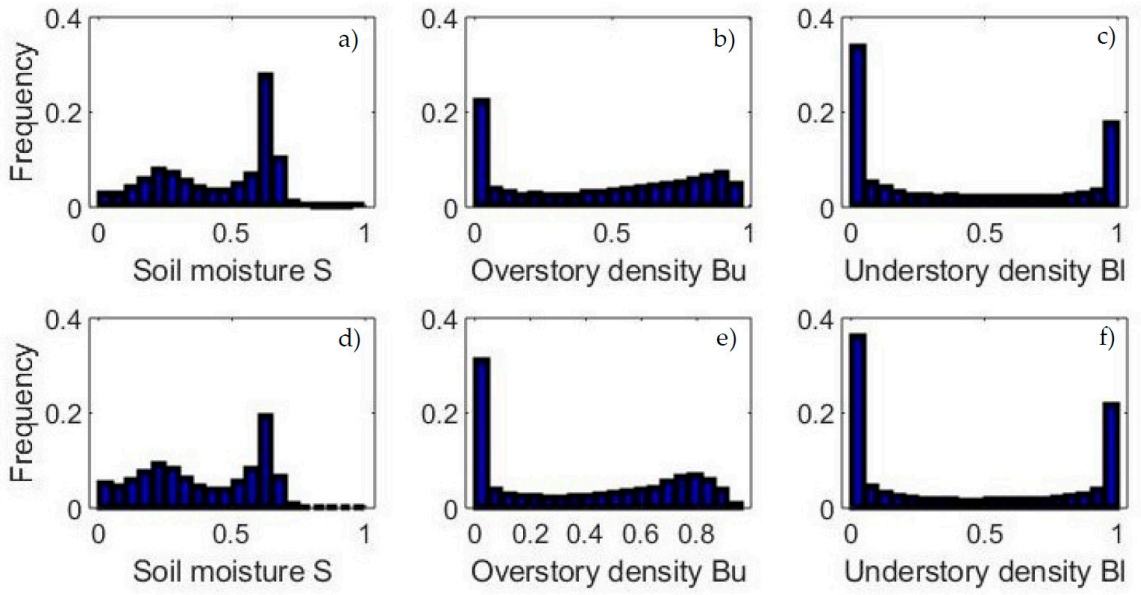

Figure 5. Frequency histograms of relative soil moisture (S; **a**,**d**), overstory density (B_u; **b**,**e**), and understory density (B_l; **c**,**f**) for precipitation scenarios S1-A (**a**–**c**) and S1-B (**d**–**f**) and for the loam (L) soil.

The panels in Figure 6 depict the frequency histograms for precipitation scenario S2 (low yearly rainfall) and a sandy clay loam (SCL) soil. Comparison of all the corresponding panels of Figures 5 and 6 highlights the effects that the soil hydraulic behavior exerts on such variables. The histograms of relative soil moisture still show a bimodality in the frequency distributions of this state variable. The panels pertaining to the plant species follow clearly different patterns: a long-right tail after dropping off sharply just after the peak at zero for the overstory vegetation, contrasting with a long-left tail and a relatively swift rise to the peak at one for the understory vegetation. Concerning the frequency histograms for the overstory, it is clear that now the scarce available rainfall (scenario S2) does not enable the tree species to recover after fire events. As may be noted on comparing the corresponding overstory density panels of Figures 5 and 6, the latter feature is exacerbated by the lower soil moisture availability provided by the SCL soil. Allowing for the different evapotranspiration characteristics of the plant species in the two vegetation types, under the condition of precipitation shortfall the hydraulic behavior of the SCL soil is able to support the understory to a greater extent, much less so the overstory.

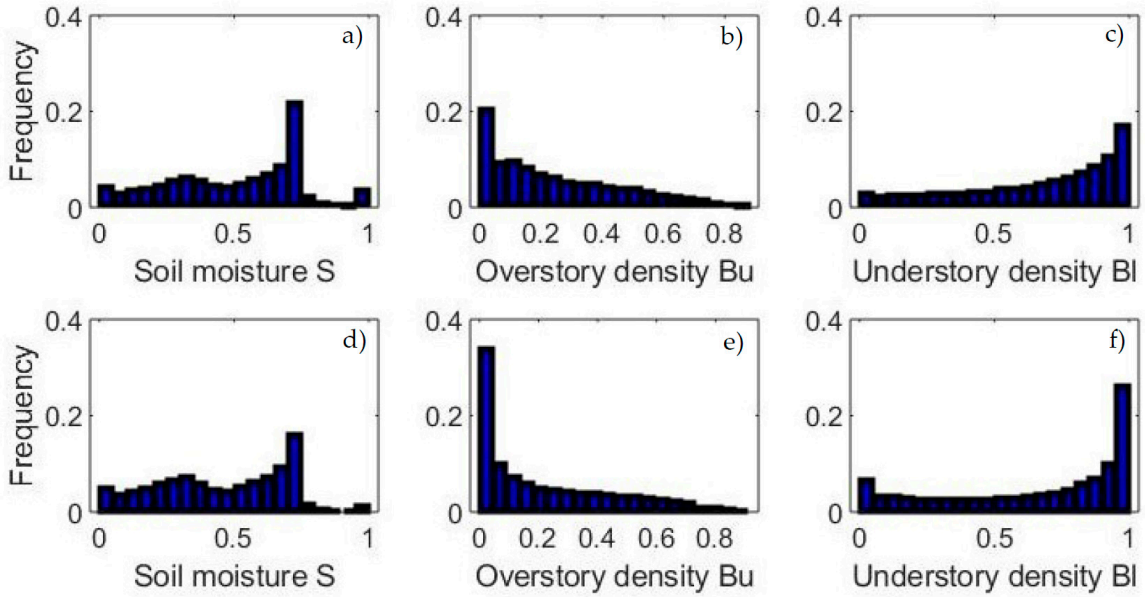

Figure 6. Frequency histograms of relative soil moisture (S; **a**,**d**), overstory density (B_u; **b**,**e**), and understory density (B_l; **c**,**f**) for precipitation scenarios S2-A (**a**–**c**) and S2-B (**d**–**f**) and for the sandy clay loam (SCL) soil.

4. Proper Framing of this Study and Concluding Remarks

There is an increase in public awareness of the complexity of the issues regarding the recurrence and intensity of certain perturbations, such as severe forest fires, and how a certain ecosystem, such as a typical Mediterranean environment, responds to them. The scientific community is required, more so than in the past, to contribute not only with improvements in the ability to forecast such phenomena, but also, and perhaps especially, to provide a better interpretation of the underlying processes. We promote a modeling framework with the main objective of highlighting the importance of looking at the problem with a long-term perspective when one has to tackle questions relating to the possible ecosystem regime shift that is generated by a strong perturbation, such as a wildfire. Even though we cannot yet guarantee an adequate validation of our approach, mostly due to the lack of a suitably long time series of fire events, we hope that our sensitivity analysis, based on well-known modeling theories, may contribute to the development of awareness toward such processes having a significant role to play in fire risk assessment. At this stage of the research development, we have demonstrated that risk assessment requires an accurate description of the hydrological forcing and soil characteristics, which are available but rarely taken into consideration when assessing fire risk.

Longer-term simulations of natural fire-prone ecosystems, such as those presented here and obtained through a zero-dimensional nonlinear ecohydrological approach coupled with a predator–prey model, are not intended to provide a real-time fire risk assessment or reproduce site-specific sequences of fire, but rather have the primary objective to investigate potential fire regime shifts that may lead an ecosystem too far from its physiological and self-sustaining dynamics which, in turn, may threaten the ecosystem itself, the society relying on it, and global equilibria. Infiltration and soil-water storage were proved to be crucial processes to determine the characteristics of fire regimes, both directly and mostly indirectly. The comprehensive model presented in this paper shed some light and unraveled the complex interaction between fire development and the variability of precipitation, especially the typical Mediterranean seasonality, the dynamics of soil moisture (as also related to specific soil properties), and biomass growth.

This case study of fire regime in the region of Campania was based on available long time-series of daily rainfall and took account of the presence of higher-frequency fluctuations between the wetter and drier seasons during the last two decades. The conceptual model that we used did not predict a

clear shift of the fire regime from the chaotic, "physiological" Mediterranean fire regime, but rather highlighted the occurrence of a redistribution of biomass between the two main vegetation layers as if the characteristics of a typical Mediterranean forest fire regime would include resilience to the observed climate change. By contrast, a previous study by Ursino and Romano [24] investigated the effects of land-use change on the dynamics of forest fires in a Mediterranean basin, based on the observed change in the partitioning between cropland and forest, showing that the land-use changes occurring over the last five decades can induce a shift in the fire regime.

In conclusion, with reference to external threats to the chaotic and self-sustaining dynamics of fire in a representative zone of the Mediterranean belt, such as the region of Campania, climate change or alterations to rainfall seasonality do not seem the most probable causes of shifts in the fire regime. Instead, drawing on the outcomes from some recent studies specifically carried out in Mediterranean areas, human activity more related to land-cover changes, alterations in land-use patterns, and degradation of terraced landscapes [57,58], may have affected the frequency and magnitude of fires recorded during the last decade to a greater extent. A relatively poor soil-water holding capacity associated with growing aridity drives the ecosystem to a progressive shift toward states of sparse tree cover, whereas good water retention characteristics of soil establish a bimodal distribution of biomass density that can be interpreted as a precursor of catastrophic shifts from forest to shrubland as the climate changes.

The results and conclusions presented herein are at present the best forecasts we can make on long-term complex processes yet to occur. They do not aim to be used for fire risk assessment, but rather as an alarm tool toward possible long-term ecosystem shifts.

Author Contributions: Conceptualization, N.R. and N.U.; Methodology, N.R. and N.U.; Software, N.R. and N.U.; Writing—review & editing, N.R. and N.U. Both authors read and agreed to the published version of the manuscript. All authors have read and agreed to the published version of the manuscript.

Funding: This research was funded, in part, by the Italian Ministry of University and Research (MiUR) within the frame of the PRIN (Progetti di Ricerca di Rilevante Interesse Nazionale—Call 2017) project "WATZON—WATer mixing in the critical ZONe: observations and predictions under environmental changes" (grant number 2017SL7ABC) and the iAQUEDUCTproject under the 2018 Joint call of the Water Works ERA-NET Co fund with the European Commission (EC) (Project number: ENWWW.2018.5).

Acknowledgments: We would like to thank Paolo Nasta and Carolina Allocca for their help in some of the calculations presented in this paper. The first author acknowledges the funding from a research agreement between the Department of Agricultural Sciences of University of Naples Federico II and Ente Parco Nazionale del Vesuvio (EPNV) about the measures to mitigate the consequences of the wildfires which occurred in Summer 2017. Finally, we thank two anonymous reviewers whose constructive comments helped improve the final version of this paper.

Conflicts of Interest: The authors declare no conflict of interest.

Appendix A

Table A1. Values of some model parameters

Variable	Value	Units	Description
Z	40	cm	Thickness of the soil control volume (see Equation (1))
Δ_u	0.25	cm	Rainfall threshold for overstory interception (see Equation (4))
Δ_l	0.080	cm	Rainfall threshold for understory interception (see Equation (4))
K_ϕ	1	-	Parameter characterizing soil wettability in a post-fire condition (see Equation (9))
S_{fire}	0.40		Soil moisture threshold for no fire (see Equation (17))
χ	0.01		Fire feedback coefficient (see Equation (17))

Table A2. Campbell soil hydraulic parameters (see Equations A1) and initial soil infiltration capacity (f_0) for a uniform soil profile with loam or sandy-clay-loam texture.

Soil Texture	θ_r	$\theta_s = n$	h_b	l	$\gamma = 2l + 3$	K_s	f_0
	($cm^3\ cm^{-3}$)	($cm^3\ cm^{-3}$)	(cm)	(-)	(-)	($cm\ day^{-1}$)	($cm\ day^{-1}$)
Loam	0.00	0.451	14.6	5.39	13.78	60.05	100.00
Sandy Clay Loam	0.00	0.420	8.63	7.12	17.24	54.43	100.00

Campbell's soil water retention and hydraulic conductivity relations employed in this study [55]:

$$\begin{cases} S(h) = \frac{\theta}{\theta_s} = \left(\frac{h_b}{h}\right)^{\frac{1}{l}} & for\ h \geq h_b \\ S(h) = \frac{\theta}{\theta_s} = 1 & otherwise \end{cases} \quad ; \quad \frac{K(\theta)}{K_s} = \left(\frac{\theta}{\theta_s}\right)^{\gamma}, \tag{A1}$$

Table A3. Soil-related characteristics for overstory (subscript *u*) and understory (subscript *l*) to identify the losses from the bucket due to soil evaporation and plant transpiration.

Soil Texture	Veg. Type	θ_h	θ_{wp}	θ^*	θ_{fc}	θ^{**}
		(-)	(-)	(-)	(-)	(-)
Loam	Overstory	0.065	0.110	0.199	0.281	
	Understory	0.065	0.100	0.210	0.281	0.221
Sandy Clay loam	Overstory	0.090	0.134	0.210	0.311	
	Understory	0.090	0.124	0.219	0.311	0.201

Table A4. Values of maximum transpiration and evaporation for overstory (subscript *u*) and understory (subscript *l*).

Vegetation Type	Period	T_{max}	E_{max}
		($mm\ day^{-1}$)	($mm\ day^{-1}$)
overstory	wet	0.00	0.00
	dry	2.81	0.65
understory	wet	0.00	0.00
	dry	0.19	0.65

Table A5. Parameter values of the vegetation characteristics for overstory (subscript *u*) and understory (subscript *l*).

Variable	Value	Unit	Description
r_u	0.25	yr^{-1}	Specific growth rate of the overstory
r_l	1.50	yr^{-1}	Specific growth rate of the understory
k_u; k_l	10	$kg\ m^{-2}$	Carrying capacities of the two biomass layers
α	0.05	$kg\ m^{-2}\ yr^{-1}$	Factor limiting growth of the understory due to interspecific competition for light
β_u; β_l	25.0; 95.0	yr^{-1}	Specific rate at which fire develops within each biomass layer
γ_u; γ_l	0.10	yr^{-1}	Specific rate at which fire spreads from one biomass layer to the other
δ_u	1/(17/365) = 21.47	yr^{-1}	Specific fire extinction rate for overstory
δ_l	1/(4/365) = 91.25	yr^{-1}	Specific fire extinction rate for understory
h; h_l; h_u	0.15	$kg\ m^{-2}$	Biomass density supporting a fire development rate one-half the maximum development rate

References

1. Gudmundsson, L.; Rego, F.C.; Rocha, M.; Seneviratne, S.I. Predicting above normal wildfire activity in southern Europe as a function of meteorological drought. *Environ. Res. Lett.* **2014**, *9*, 084008. [CrossRef]
2. Hanel, M.; Rakovec, O.; Markonis, Y.; Máca, P.; Samaniego, L.; Kyselý, J.; Kumar, R. Revisiting the recent European droughts from a long-term perspective. *Sci. Rep.* **2018**, *8*, 9499. [CrossRef] [PubMed]
3. Miralles, D.G.; Gentine, P.; Seneviratne, S.I.; Teuling, A.J. Land-atmospheric feedbacks during droughts and heatwaves: State of the science and current challenges. *Ann. N. Y. Acad. Sci.* **2018**, *1436*, 19–35. [CrossRef]
4. Barros, A.M.G.; Pereira, J.M.C. Wildfire selectivity for land cover type: Does size matter? *PLoS ONE* **2014**, *9*, e84760. [CrossRef]
5. Doerr, S.H.; Santín, C. Global trends in wildfire and its impacts: Perceptions versus realities in a changing world. *Philos. Trans. R. Soc. B* **2016**, *371*, 20150345. [CrossRef]
6. Romano, N. Intertwining observations and predictions in vadose zone hydrology: A review of selected studies. *Water* **2020**, *12*, 1107. [CrossRef]
7. Nasta, P.; Palladino, M.; Sica, B.; Pizzolante, A.; Trifuoggi, M.; Toscanesi, M.; Giarra, A.; D'Auria, J.; Nicodemo, F.; Mazzitelli, C.; et al. Evaluating pedotransfer functions for predicting soil bulk density using hierarchical mapping information in Campania, Italy. *Geoderma Reg.* **2020**, *21*, e00267. [CrossRef]
8. Eagleson, P.S. *Dynamic Hydrology*; EGU Reprint Series, #2; Copernicus GmbH: Katlenburg-Lindau, Germany, 2003; ISBN 3-936586-09-8.
9. Rodríguez-Iturbe, I.; Porporato, A. *Ecohydrology of Water-Controlled Ecosystems: Soil Moisture and Plant Dynamics*; Cambridge University Press: New York, NY, USA, 2004; p. 442. ISBN 0521819431.
10. Keeley, J.E.; Bond, W.J.; Bradstock, R.A.; Pausas, J.G.; Rundel, P.W. *Fire in Mediterranean Ecosystems: Ecology, Evolution and Management*; Cambridge University Press: New York, NY, USA, 2012; p. 522. ISBN 9780521824910.
11. Turco, M.; Llasat, M.C.; Tudela, A.; Castro, X.; Provenzale, A. Decreasing fires in a Mediterranean region (1970–2010, NE Spain). *Nat. Hazards Earth Syst. Sci.* **2013**, *13*, 649–652. [CrossRef]
12. Turco, M.; von Hardenberg, J.; AghaKouchak, A.; Llasat, M.C.; Provenzale, A.; Trigo, R.M. On the key role of droughts in the dynamics of summer fires in Mediterranean Europe. *Sci. Rep.* **2017**, *81*, 1–10. [CrossRef]
13. Seidl, R.; Thom, D.; Kautz, M.; Martin-Benito, D.; Peltoniemi, M.; Vacchiano, G.; Wild, J.; Ascoli, D.; Petr, M.; Honkaniemi, J.; et al. Forest disturbances under climate change. *Nat. Clim. Chang.* **2017**, *7*, 395–402. [CrossRef]
14. Camia, A.; Amatulli, G. Weather factors and fire danger in the Mediterranean. In *Earth Observation of Wildland Fires in Mediterranean Ecosystems*; Chuvieco, E., Ed.; Springer: Berlin/Heidelberg, Germany, 2009; pp. 71–82.
15. Seidl, R.; Fernandes, P.M.; Fonseca, T.F.; Gillet, F.; Jönssong, A.M.; Merganičováh, K.; Netherer, S.; Arpaci, A.; Bontemps, J.-D.; Bugmann, H.; et al. Modelling natural disturbances in forest ecosystems: A review. *Ecol. Model.* **2011**, *222*, 903–924. [CrossRef]
16. Thuiller, W.; Slingsby, J.A.; Privett, S.D.J.; Cowling, R.M. Stochastic species turnover and stable coexistence in a species-rich, fire-prone plant community. *PLoS ONE* **2007**, *2*, e938. [CrossRef]
17. De Bano, L.F. The role of fire and soil heating on water repellency in wildland environments: A review. *J. Hydrol.* **2000**, *231*, 195–206. [CrossRef]
18. Bond, W.J.; Keeley, J.E. Fire as a global "herbivore": The ecology and evolution of flammable ecosystems. *Trends Ecol. Evol.* **2005**, *20*, 387–394. [CrossRef] [PubMed]
19. Rodríguez-Iturbe, I.; D'Odorico, P.; Porporato, A.; Ridolfi, L. Tree-grass coexistence in Savannas: The role of spatial dynamics and climate fluctuations. *Geophys. Res. Lett.* **1999**, *26*, 247–250. [CrossRef]
20. Romano, N.; Palladino, M.; Chirico, G.B. Parameterization of a bucket model for soil-vegetation-atmosphere modeling under seasonal climatic regimes. *Hydrol. Earth Syst. Sci.* **2011**, *15*, 3877–3893. [CrossRef]
21. Feng, X.; Ackerly, D.D.; Dawson, T.E.; Manzoni, S.; Skelton, R.P.; Vico, G.; Thompson, S.E.; Maherali, H. The ecohydrological context of drought and classification of plant responses. *Ecol. Lett.* **2018**, *21*, 1723–1736. [CrossRef]
22. Lasaponara, R.; Santulli, A.; Telesca, L. Time-clustering analysis of forest-fire sequences in southern Italy. *Chaos Soliton. Fract.* **2005**, *24*, 139–149. [CrossRef]
23. Ursino, N.; Rulli, M.C. Hydrological minimal model for fire regime assessment in a Mediterranean ecosystem. *Water Resour. Res.* **2011**, *47*, W11526. [CrossRef]

24. Ursino, N.; Romano, N. Wild forest fire regime following land abandonment in the Mediterranean region. *Geophys. Res. Lett.* **2014**, *41*, 8359–8368. [CrossRef]
25. Platt, W.J.; Orzell, S.L.; Slocum, M.G. Seasonality of fire weather strongly influences fire regimes in South Florida savanna-grassland landscapes. *PLoS ONE* **2015**, *10*, e0116952. [CrossRef] [PubMed]
26. Guswa, A.J.; Celia, M.A.; Rodriguez-Iturbe, I. Models of soil moisture dynamics in ecohydrology: A comparative study. *Water Resour. Res.* **2002**, *38*, W01166. [CrossRef]
27. Porporato, A.; D'Odorico, P.; Laio, F.; Ridolfi, L.; Rodriguez-Iturbe, I. Ecohydrology of water-controlled ecosystems. *Adv. Water Res.* **2002**, *25*, 1335–1348. [CrossRef]
28. De Groen, M.M.; Savenije, H.H.G. A monthly interception equation based on the statistical characteristics of daily rainfall. *Water Resour. Res.* **2006**, *42*, W12417. [CrossRef]
29. Caylor, K.K.; D'Odorico, P.; Rodriguez-Iturbe, I. On the ecohydrology of structurally heterogeneous semiarid landscapes. *Water Resour. Res.* **2006**, *42*, W07424. [CrossRef]
30. Cerdà, A.; Robichaud, P.R. Fire effects on soil infiltration. In *Fire Effects on Soils and Restoration Strategies*; Cerdà, A., Robichaud, P.R., Eds.; Science Publishers: Enfield, NH, USA, 2009; Volume 5, pp. 81–103.
31. Larsen, I.J.; MacDonald, L.H.; Brown, E.; Rough, D.; Welsh, M.J.; Pietraszek, J.H.; Libohova, Z.; de Dios Benavides-Solorio, J.; Schaffrath, K. Causes of post-fire runoff and erosion: The roles of soil water repellency, surface cover, and soil sealing. *Soil Sci. Soc. Am. J.* **2009**, *73*, 1393–1407. [CrossRef]
32. Doerr, S.H.; Shakesby, R.A.; Walsh, R.P.D. Soil water repellency: Its causes, characteristics and hydro-geomorphological significance. *Earth-Sci. Rev.* **2000**, *51*, 33–65. [CrossRef]
33. Letey, J. Causes and consequences of fire-induced soil water repellency. *Hydrol. Process.* **2001**, *15*, 2867–2875. [CrossRef]
34. Pierson, F.B.; Robichaud, P.R.; Moffet, C.A.; Spaeth, K.E.; Hardegree, S.P.; Clark, P.E.; Williams, C.J. Fire effects on rangeland hydrology and erosion in a steep sagebrush-dominated landscape. *Hydrol. Process.* **2008**, *22*, 2916–2929. [CrossRef]
35. Ravi, S.; D'Odorico, P.; Wang, L.; White, C.S.; Okin, G.S.; Macko, S.A.; Collins, S.L. Post-fire resource redistribution in desert grasslands: A possible negative feedback on land degradation. *Ecosystems* **2009**, *12*, 434–444. [CrossRef]
36. Mataix-Solera, J.; Cerdà, A.; Arcenegui, V.; Jordán, A.; Zavala, L.M. Fire effects on soil aggregation: A review. *Earth-Sci. Rev.* **2011**, *109*, 44–60. [CrossRef]
37. Prosser, I.P.; Williams, L. The effect of wildfire on runoff and erosion in native Eucalyptus forest. *Hydrol. Process.* **1998**, *12*, 251–265. [CrossRef]
38. Robichaud, P.R.; Beyers, J.L.; Neary, D.G. *Evaluating the Effectiveness of Postfire Rehabilitation Treatments*; Gen. Tech. Rep. RMRS-GTR-63; U.S. Department of Agriculture, Forest Service, Rocky Mountain Research Station: Fort Collins, CO, USA, 2000; pp. 1–89.
39. Choromanska, U.; De Luca, T.H. Prescribed fire alters the impact of wildfire on soil biochemical properties in a ponderosa pine forest. *Soil Sci. Soc. Am. J.* **2001**, *65*, 232–238. [CrossRef]
40. Mayor, A.G.; Bautista, S.; Llovet, J.; Bellot, J. Post-fire hydrological and erosional responses of a Mediterranean landscape: Seven years of catchment-scale dynamics. *Catena* **2007**, *71*, 68–75. [CrossRef]
41. Capitanio, R.; Carcaillet, C. Post-fire Mediterranean vegetation dynamics and diversity: A discussion of succession models. *For. Ecol. Manag.* **2008**, *255*, 431–439. [CrossRef]
42. Allen, R.G.; Pruitt, W.O.; Raes, D.; Smith, M.; Pereira, L.S. Estimating evaporation from bare soil and the crop coefficient for the initial period using common soils information. *J. Irrig. Drain. Eng.* **2005**, *131*, 14–23. [CrossRef]
43. Nasta, P.; Romano, N. Use of a flux-based field capacity criterion to identify effective hydraulic parameters of layered soil profiles subjected to synthetic drainage experiments. *Water Resour. Res.* **2016**, *52*, 566–584. [CrossRef]
44. Henley, C.L. Statics of a "self-organized" percolation model. *Phys. Rev. Lett.* **1993**, *71*, 2741–2744. [CrossRef]
45. Sutherland, B.R.; Jacobs, A.E. Self-organization and scaling in a lattice predator-prey model. *Complex Syst.* **1994**, *8*, 385–405.
46. Casagrandi, R.; Rinaldi, S. A minimal model for forest fire regimes. *Am. Nat.* **1999**, *153*, 527–539. [CrossRef]
47. Melillo, J.M.; McGuire, A.D.; Kicklighter, D.W.; Moore, B.; Vorosmarty, C.J.; Schloss, A.L. Global climate change and terrestrial net primary production. *Nature* **1993**, *363*, 234–240. [CrossRef]

48. Olsen, J.M. *Cistus, Fuel Moisture and Flammability*; Research Note #159; USDA, California Forest and Range Experiment Station: Berkeley, CA, USA, 1960.
49. Countryman, C.M.; Dean, W.A. *Measuring Moisture Content in Living Chaparral: A Field User's Manual*; Gen. Tech. Rep. PSW-36; Pacific South West Forest and Range Exp. Stn., Forest Serv., U.S. Department of Agriculture: Berkeley, CA, USA, 1979; pp. 1–27.
50. Dennison, P.E.; Roberts, D.A.; Thorgusen, S.R.; Regelbrugge, J.C.; Weise, D.; Lee, C. Modeling seasonal changes in live fuel moisture and equivalent water thickness using a cumulative water balance index. *Remote Sens. Environ.* **2003**, *88*, 442–452. [CrossRef]
51. Dennison, P.E.; Roberts, D.A.; Peterson, S.H.; Rechel, J. Use of normalized difference water index for monitoring live fuel moisture. *Int. J. Remote Sens.* **2005**, *26*, 1035–1042. [CrossRef]
52. Peterson, S.H.; Goldstein, N.C.; Clark, M.L.; Halligan, K.Q.; Schneider, P.; Dennison, P.E.; Roberts, D.A. Sensitivity analysis of a model of the 2003 simi wildfire event. In *Proceedings of the 8th Interantional Conference on GeoComputation, Ann Arbor, MI, USA, 31 July–3 August 2005*; Xie, Y., Brown, D.G., Eds.; GeoComputation CD-ROM: Ann Arbor, MI, USA, 2005; Available online: http://www.geocomputation.org/2005/ (accessed on 1 September 2020).
53. Walsh, R.P.D.; Lawler, D.M. Rainfall seasonality: Description, spatial patterns and change through time. *Weather* **1981**, *36*, 201–208. [CrossRef]
54. World Meteorological Organization (WMO); Global Water Partnership (GWP). *Handbook of Drought Indicators and Indices*; IDMP, IDM Tools and Guidelines, Series 2; Svoboda, M., Fuchs, B.A., Eds.; World Meteorological Organization: Geneva, Switzerland, 2016.
55. Campbell, G.S. A simple method for determining unsaturated conductivity from moisture retention data. *Soil Sci.* **1974**, *117*, 311–314. [CrossRef]
56. Nasta, P.; Allocca, C.; Deidda, R.; Romano, N. Assessing the impact of seasonal rainfall anomalies on catchment-scale water balance components. *Hydrol. Earth Syst. Sci.* **2020**, *24*, 3211–3227. [CrossRef]
57. Tarolli, P.; Preti, F.; Romano, N. Terraced landscapes: From an old best practice to a potential hazard for soil degradation due to land abandonment. *Anthropocene* **2014**, *6*, 10–25. [CrossRef]
58. Nasta, P.; Palladino, M.; Ursino, N.; Saracino, A.; Sommella, A.; Romano, N. Assessing long-term impact of land-use change on hydrological ecosystem functions in a Mediterranean upland agro-forestry catchment. *Sci. Total. Environ.* **2017**, *605*, 1070–1082. [CrossRef]

© 2020 by the authors. Licensee MDPI, Basel, Switzerland. This article is an open access article distributed under the terms and conditions of the Creative Commons Attribution (CC BY) license (http://creativecommons.org/licenses/by/4.0/).